

TESS3: Fast Inference of Spatial Population Structure and Genome Scans for Selection

Kevin Caye¹ Timo M. Deist¹ Helena Martins¹ Olivier Michel²
Olivier François¹

¹Université Grenoble-Alpes, Centre National de la Recherche Scientifique, TIMC-IMAG UMR
5525, Grenoble, 38042, France.

²Université Grenoble-Alpes, Centre National de la Recherche Scientifique, GIPSA-lab UMR
5216, Grenoble, 38042, France.

Running Title: TESS3: Inference of Spatial Population Structure

Keywords: Inference of Population Structure, Geographic Variation, Genome Scans for Selection,
Control of False Discoveries.

Corresponding Author: Olivier François

Université Grenoble-Alpes,
TIMC-IMAG, UMR CNRS 5525,

Grenoble, 38042, France.

+334 56 52 00 25 (ph.)

+334 56 52 00 55 (fax)

olivier.francois@imag.fr

Abstract

Geography and landscape are important determinants of genetic variation in natural populations, and several ancestry estimation methods have been proposed to investigate population structure using genetic and geographic data simultaneously. Those approaches are often based on computer-intensive stochastic simulations, and do not scale with the dimensions of the data sets generated by high-throughput sequencing technologies. There is a growing demand for faster algorithms able to analyze genome-wide patterns of population genetic variation in their geographic context.

In this study, we present TESS3, a major update of the spatial ancestry estimation program TESS. By combining matrix factorization and spatial statistical methods, TESS3 provides estimates of ancestry coefficients with accuracy comparable to TESS and with run-times much faster than the Bayesian version. In addition, the TESS3 program can be used to perform genome scans for selection, and separate adaptive from non-adaptive genetic variation using ancestral allele frequency differentiation tests. The main features of TESS3 are illustrated using simulated data and analyzing genomic data from European lines of the plant species *Arabidopsis thaliana*.

1 Introduction

Since the early developments of population genetics, geography has been recognized as one of the major determinants of genetic variation in natural populations (Wright, 1943; Malécot, 1948; Kimura & Weiss, 1964; Cavalli-Sforza *et al.*, 1994; Epperson, 2003). For these populations, spatial patterns of genetic variation can be influenced by landscape barriers, geographical distances and by the processes of divergence and admixture resulting from the colonization of new areas. In addition, analyzing spatial patterns of genetic variation has been a long-standing goal of evolutionary biogeography, molecular ecology, landscape genetics, and conservation biology (Segelbacher *et al.*, 2010; Manel *et al.*, 2010).

Statistical approaches to analyze spatial patterns of genetic variation often rely on the inference of population genetic structure from multi-locus genotype data, which is commonly performed using the Bayesian approach implemented in the computer program **STRUCTURE** (Pritchard *et al.*, 2000). Assuming K unobserved ancestral gene pools, **STRUCTURE** computes allele frequencies in each pool, and estimates individual *ancestry coefficients* representing the proportion of an individual genome that originates from each pool. Using **STRUCTURE**, ancestry coefficients are estimated without prior knowledge on geographic proximity among individuals.

The approach implemented in **STRUCTURE** has been substantially improved by a number of approaches that include spatial proximity information based on individual geographic coordinates (reviewed by François & Durand (2010)). Among those spatially explicit approaches, the computer program **TESS** is one of the most frequently used algorithms (Chen *et al.*, 2007; François *et al.*, 2006). In the **TESS** model, ancestry proportions are continuously distributed over geographic space, and the parameters that specify the shape of the clines are estimated from the genetic and the geographic data. Using geographic information, **TESS** provides better estimates of ancestry coefficients than **STRUCTURE** when the levels of ancestral population divergence are low (Durand *et al.* 2009).

The Bayesian approaches implemented in **STRUCTURE** and **TESS** rely on Markov Chain Monte Carlo algorithms. Monte Carlo algorithms are based on computer intensive stochastic simulations, and have the advantage of sampling the posterior distribution of the model parameters. However

the application of stochastic algorithms can be difficult when the data include more than a few hundreds of individuals or a few thousands of allelic markers. With the availability of next generation sequencing data, there is a need to analyze genotypic matrices that represent thousands of individuals and hundreds of thousands of markers. While fast versions of **STRUCTURE** have already been proposed (Raj *et al*, 2014; Fritchot *et al*, 2014; Alexander & Lange, 2011; Wollstein & Lao, 2015), developing fast and accurate estimation algorithms for ancestry coefficients in a geographic framework remains an important computational challenge.

In this study, we present a spatially explicit algorithm that provides fast estimation of ancestry coefficients with accuracy comparable to **TESS** 2.3 (Durand *et al*, 2009). The new algorithms are based on least-squares optimization and on geographically constrained non-negative matrix factorization (Cai *et al*, 2011; Fritchot *et al*, 2014). These improvements of **TESS** are implemented in the computer program **TESS3**. We show that **TESS3** is substantially faster than **TESS** 2.3, with an increase in computational speed of one or two orders of magnitude. In addition, we show that ancestral allele frequencies are correctly estimated, and we illustrate the use of the **TESS3** program to perform genome scans for selection based on ancestral allele frequency differentiation. To illustrate our approach, **TESS3** was applied to genomic data from European lines of the model species *Arabidopsis thaliana* for which an individual-based sampling design was available (Atwell *et al*, 2010).

2 Materials and Methods

The computer program **TESS3** computes ancestry estimates for large genotypic matrices using the geographic coordinates of sampled individuals. The program also returns locus-specific estimates of ancestral genotypic frequencies, and computes locus-specific estimates of a population-based differentiation statistic that can be used in genome scans for adaptive alleles. The **TESS3** program is particularly suited to the analysis of large genomic data sets, for which the number of loci (L) ranges between thousands to hundreds of thousands genetic polymorphisms and the number of individuals (n) ranges between hundreds to thousands individuals.

Input data. TESS3 requires that the data consists of n multi-locus genotypes and two geographic coordinates for each genotype. A genotypic matrix, X , records allelic data for each individual (i) and each locus (ℓ). With data representing single nucleotide polymorphisms (SNPs), the genotypic matrix records the number of derived or mutant alleles at each locus. Considering autosomes in a diploid organism, the genotype at locus ℓ corresponds to the number of derived alleles at this locus, which is encoded as an integer number 0, 1 or 2. For SNPs, the `geno` format is accepted by the program, which can also process other types of allelic data, such as short tandem repeats or amplified fragment length polymorphisms. Geographic coordinates can be expressed using several coordinate systems, for example longitude and latitude, and they are provided to the software in a separate input file.

Geographically constrained least-squares estimates of ancestry coefficients. Similarly to TESS 2.3 or STRUCTURE, TESS3 supposes that the genetic data originate from the admixture of K ancestral populations, where K is unknown. TESS3 estimates a Q -matrix, $Q = (Q_{ik})$, which represents the individual ancestry coefficients ($n \times K$ dimensions), and a G -matrix, $G = (G_{k\ell}(j))$, which represents the ancestral genotypic frequencies. The dimension of G is equal to $K \times (p+1)L$ where p is the ploidy of the studied organism genome. The ancestry coefficient Q_{ik} is the fraction of individual i 's genome that originates from the ancestral population k , and the coefficient $G_{k\ell}(j)$ represents the frequency of genotype j at locus ℓ in population k .

The principle underlying the TESS3 algorithm differs from the likelihood methods implemented in STRUCTURE or in TESS 2.3, and it can be considered to be model-free. The main idea is that the probability that an individual i carries the genotype j at locus ℓ is determined by the *law of total probability*

$$P(X_{i\ell} = j) = \sum_{k=1}^K Q_{ik} G_{k\ell}(j).$$

The above formula establishes that each individual genotype is sampled from K pools of ancestral genotypes, and that the sampling probabilities correspond to their admixture coefficients. The formula is equivalent to the factorization of the genotypic probability matrix, P , using the matrices Q and G as factors (Frichot *et al*, 2014). In the TESS3 algorithm, probabilities are

replaced by zero/one values depending on the absence or the presence of each genotype at each locus, and the resulting matrix is denoted by \tilde{X} . Estimates of Q and G are obtained by factorizing \tilde{X} as follows $\tilde{X} = \hat{Q}\hat{G}$. Matrix factorization is performed according to a least-squares minimization algorithm (see Appendix). During the minimization process, spatial constraints are introduced to ensure that individuals that are geographically close to each other are more likely to share the same ancestral genotypes than individuals that are far apart. A regularization parameter, α , controls the regularity of ancestry estimates over the geographic space. Large values of α imply that ancestry coefficients have similar values for nearby individuals, whereas small values produce results close to **STRUCTURE**. The least-squares method leads to algorithms that are substantially faster than the Bayesian algorithms implemented in other programs. In addition, the approach makes no assumptions about linkage or Hardy-Weinberg equilibrium (HWE). The above framework is thus appropriate to deal with departures from HWE created by inbreeding or geographically restricted mating.

Number of populations. In TESS3, the number of ancestral populations, K , is chosen after the evaluation of a cross-entropy criterion for each K (Frichot *et al*, 2014). The choice of K is then based on a cross-validation method that partitions the genotypic matrix entries into a training set and a test set in which 5% of all entries are masked to the algorithm. The cross-entropy criterion compares the genotypic frequencies predicted from the training set to those computed from the test set at each locus. Smaller values of the criterion often indicate better estimates for TESS3. In practice, the best choice for K corresponds to a plateau in the cross-entropy plot (Frichot & François, 2015)..

Outlier locus tests. In addition to the inference of spatial population structure, TESS3 can perform genome scans for selection when the program is applied to large genomic data sets. More specifically, TESS3 uses the ancestral genotype frequency matrix, G , to derive the allele frequencies in the K ancestral populations. Then the algorithm evaluates a locus-specific F_{ST} -statistic based on the estimated ancestral allele frequencies. Using standard population genetic theory, F_{ST} -statistics can be transformed into squared z -scores, and p -values can be computed

using a chi-square distribution with $K - 1$ degrees of freedom (Weir, 1996). To correct for the test inflation statistic due to neutral population structure, the z -scores were recalibrated using estimates of the inflation factor. Here, inflation factors were determined using an “empirical-null hypothesis” approach. The values of the inflation factor were determined graphically on the basis on quantile-quantile plots of p -values. This approach is less conservative than the method based on the median of the chi-square distribution with $K - 1$ degrees of freedom (Devlin & Roeder, 1999; Frichot & François, 2015). Multiple testing issues were addressed by applying the Benjamini-Hochberg algorithm to the recalibrated p -values (Benjamini & Hochberg, 1995).

Simulated data sets and program runs. We created simulated data sets containing 200 admixed genotypes with levels of ancestry that varied continuously across geographic space. To generate the data, we used the computer program `MS` to perform coalescent simulations of neutral and outlier SNPs under island models with two populations (Hudson, 2002). One hundred genotypes were sampled from each source population, and admixed genotypes were created according to a longitudinal gradient of ancestry (Durand *et al*, 2009; François & Durand, 2010). Individuals at each extreme of the longitudinal range were representative of ancestral populations, while individuals at the center of the range shared intermediate levels of ancestry in the two source populations. The number of loci was varied in the range $L = 1\text{k}-50\text{k}$ SNPs.

Our first series of simulations considered selectively neutral SNPs and used migration parameters, $M = 4mN_e$, between $M = 0.01$ and $M = 10$. The population differentiation statistic, F_{ST} , ranged from 0.007 to 0.42. Our second series of simulations included a proportion of outlier SNPs equal to 5%. Outlier loci were generated using two values of the effective migration rate $4m_s N = 0.1$ and $4m_s N = 1$. In simulations with outlier loci, the neutral migration rate was set to the value $4mN = 20$. The justification for using neutral migration-drift equilibrium models for simulating selection is that loci with selection have an effectively reduced migration rate, as compared to the neutral migration m in migration-selection-drift equilibrium models (Bazin *et al*, 2010).

The simulated data were used to compare TESS3 estimates to those of TESS 2.3 (Durand *et al*, 2009). The number of ancestral populations ranged from $K = 1$ to $K = 6$. Each run was

replicated five times for each computer program. The number of cycles in the Markov chain Monte Carlo algorithm of **TESS** 2.3 was set to 1,000, and the optimal number of ancestral population was determined using the deviance information criterion. All other parameters were set to their default values. Statistical errors were measured as root mean squared errors (RMSE) between the estimated Q -matrix and the matrix of coefficients (Q^0) that were used to generate the data

$$\text{RMSE} = \left(\frac{1}{nK} \sum_{i=1}^n \sum_{k=1}^K (Q_{ik} - Q_{ik}^0)^2 \right)^{1/2}.$$

A similar RMSE criterion was defined for comparing the estimates of G matrices obtained from **TESS3** or **TESS** 2.3 to the estimates of the ancestral genotypic frequency matrix resulting from the coalescent simulations.

***Arabidopsis thaliana* data.** We applied **TESS3** to genomic data from 170 European lines of the model plant *Arabidopsis thaliana* genotyped for 216k SNPs (Atwell *et al*, 2010). For these data, we determined the number of ancestral populations using the cross-entropy criterion, and we computed ancestry estimates for the sample. The results were projected onto a map of the European continent using a raster file and R graphic functions (Jay *et al*, 2012). We also used **TESS3** to perform a genome scan for selection on chromosome 5 using $K = 3$ ancestral populations (54k SNPs).

3 Results

Comparison of ancestry estimates. We used computer simulations of admixed populations to evaluate the ability of **TESS3** to reproduce the ancestry estimates of **TESS** 2.3 using known individual ancestry proportions from two ancestral gene pools. Simulating 2k unlinked SNPs, we varied the level of ancestral population differentiation, measured by F_{ST} , to create difficult as well as easier data sets. For all data sets, the information criterion of each version of **TESS** led to $K = 2$ clusters. Statistical errors, measured by RMSEs for estimated Q and G matrices, ranged between 0.02 and 0.15 (Figure 1). Statistical errors increased as the levels of differentiation between the two source populations decreased, but they remained in an acceptable range for values of F_{ST} greater than 0.016. Overall, the statistical performances were of the same order for both versions

of TESS.

Run-time analysis. Next we compared the run-times of TESS3 and TESS 2.3 for increasing values of the number of ancestral populations and increasing numbers of loci. For TESS 2.3 the total number of cycles in the MCMC algorithm was set to 1,000, a value for which the Monte-Carlo sampler reached its equilibrium state. Run-times were averaged over distinct random seed values for each K and number of loci. For both algorithms, the run-times increased with the number of loci and with the number of ancestral populations (Figure 2). For $L = 10k$ loci, TESS3 and TESS 2.3 runs took less than 6 minutes on an Intel Xeon 2.40 GHz CPU. With $L = 50k$ loci and $K = 5$ ancestral populations, TESS 2.3 took on average 30 minutes to complete a single run, whereas the TESS3 average run-time was about 4 minutes.

Outlier locus tests. We evaluated the capacity of TESS3 to detect outlier loci on simulated data containing 5% of outlier loci. For each locus, we performed a population differentiation test based on the estimated ancestral allele frequencies. Although the ratios m_s/m took large values, the probability distributions of F_{ST} statistics computed from neutral and selected ancestral allele frequencies overlapped substantially. Thus the power of neutrality tests were expected to be low. For a data set with $m_s/m = 0.005$, the estimate of the genomic inflation factor was equal to $\lambda = 4.4$. For a data set with $m_s/m = 0.05$ this value was equal to $\lambda = 10.0$. After correction of the test statistic, the observed levels of the false discovery rate were close to their expected values. The power to reject the null hypothesis was lower when the intensity of selection was low (Table 1). For an expected FDR of $q = 0.1$, the power of the test was approximately equal to 60% for the higher selection rate and it was equal to 30% for the lower selection rate. The power values were close to those obtained when we applied outlier tests to the data before admixture. This experiment showed that the power to reject neutrality in continuous populations was similar to the power of traditional population differentiation tests applied to the discrete (ancestral) population data.

Biological data analysis. We applied TESS3 to a genomic data set of 170 European lines of *Arabidopsis thaliana* (216k SNPs). The cross-entropy curve exhibited a change in curvature for

$K = 3$ - 4 clusters. For $K = 3$, the western cluster grouped all lines from the British Isles, France and Iberia. The eastern cluster grouped all lines from Central, Eastern Europe and Southern Sweden. Fourteen northern Scandinavian accessions were grouped into a separate population (Figure 3A). Those results were consistent with those obtained with TESS 2.3. The average run-time of TESS3 was about 5 minutes whereas each TESS 2.3 run took about 2 hours. Then we performed a genome scan for selection based on population differentiation in the three ancestral populations detected by TESS3. The genomic inflation factor was equal to $\lambda = 15.0$. The histogram of corrected p -values provided evidence that confounding errors were correctly removed (Figure 4A). The Manhattan plot exhibited islands of strong differentiation around positions 8,510 kb, 6,944 kb, 6,969 kb and 26,155 kb in the chromosome 5 (Figure 3B). The top hits in the candidate list corresponded to genic SNPs. In particular, we discovered genes involved in defense response (*VSP1*), and in photoperiodism, flowering and root development (*WAV2*) (Mochizuki *et al*, 2005). The derived allele in the *VSP1* gene was present at high frequency in Eastern Europe and it was almost absent from Western Europe and Northern Scandinavia. The derived allele in the *WAV2* gene was present at high frequency in the Iberian peninsula and at low frequency in Eastern Europe and Northern Scandinavia (Figure 4B).

4 Discussion

A fundamental objective of evolutionary biology is the evaluation of the distribution of genetic variation among populations in geographic space. During the last few years, high-throughput sequencing technologies have allowed population geneticists to make fast progress in this direction. The access to extensive data have opened the door to a deeper understanding of the spatial distribution of adaptive and nonadaptive genetic variation in model and non-model organisms (Manel *et al*, 2010). This transition from population genetics to population and ecological genomics is accompanied by a revolution of the principles and methods used to analyze the influence of landscape features on genetic variation. This revolution is made possible thanks to the availability of fast computing programs than can deal with high dimension and heterogeneity in the data.

By combining matrix factorization and spatial statistical methods, the computer program TESS3 enabled fast analysis of geographic and genome-wide patterns of genetic variation from

large genomic data sets. In coalescent simulations of individuals with known ancestry, TESS3 produced accurate estimates of ancestry coefficients and ancestral allele frequencies. TESS3 results were statistically similar to those obtained with the Bayesian clustering program TESS 2.3, but TESS3 was about 30 times faster than TESS 2.3 when used with $K = 5$ ancestral populations and 50k binary loci. Though Bayesian approaches might be preferable for genotypic matrices of moderate dimensions, TESS3 generally outperformed TESS 2.3 when more than a few thousands of markers were used.

A novelty of TESS3 is the identification of outlier loci from the genotypic matrix. An important property of TESS3 outlier tests is that they do not require predefined populations, and that can be applied to individual sampling designs. Based on the estimations of the ancestral allele frequency matrix, the TESS3 algorithm computes a population differentiation statistic estimating a fixation index for each locus. If local adaptation favors a particular allele in some ancestral populations, the population differentiation statistic at that locus will be larger than at loci that are selectively neutral. Outliers in the distribution of the population differentiation statistic are usually considered as loci potentially targeted by local selection (Holsinger & Weir, 2009). In addition, the program output allows population geneticists to determine candidate loci based on classical FDR control algorithms.

The study of European lines of *A. thaliana* illustrated the main steps of analysis using TESS3. These steps can be summarized as follows: 1) Identifying the number of clusters using the cross-validation criterion, by launching multiple runs of the program for each value of K , 2) Displaying maps of ancestry coefficients using R scripts provided with the program, 3) Performing a genome scan for selection based on ancestral allele frequency differentiation statistics. Results for *A. thaliana* suggested that clinal variation occurs along an East-West gradient separating two ancestral populations in Central Europe. Those results were in very good agreement with previous findings using TESS 2.3, although these findings were obtained with a different set of markers (Fran ois *et al*, 2008). A genome scan for selection revealed contrasted patterns among European lines of *A. thaliana* and provided evidence of a substantial role for natural selection in shaping the genome-wide variation of the plant species in Europe.

To conclude, the computer program TESS3 provides a major update of the TESS program enabling rapid ancestry coefficient estimation and genome scans for adaptive alleles. While preserving the accuracy of TESS 2.3, the least-squares algorithms of TESS3 ran substantially faster than the Bayesian algorithms of TESS when analyzing large population genomic data sets.

Data Accessibility

Installing TESS3. Source codes, installation files and program documentation are available from Github (<https://github.com/cayek/TESS3>).

The Atwell et al. (2010) data used in this study are publicly available from the following link:
<https://github.com/Gregor-Mendel-Institute/atpolydb>

Acknowledgments

This work was supported by a grant from the Laboratoire d'Excellence Labex Persyval-lab to Kevin Caye. H. Martins acknowledges support from the “Ciências sem Fronteiras” scholarship program from the Brazilian government. Olivier François acknowledges support from Grenoble INP, and from the “Agence Nationale de la Recherche” (project AFRICROP ANR-13-BSV7-0017).

References

- Alexander DH, Lange K (2011) Enhancements to the ADMIXTURE algorithm for individual ancestry estimation. *BMC bioinformatics*, **12**, 246.
- Atwell S, Huang YS, Vilhjálmsson BJ, *et al* (2010) Genome-wide association study of 107 phenotypes in *Arabidopsis thaliana* inbred lines. *Nature*, **465**, 627–631.
- Bazin E, Dawson KJ, Beaumont MA (2010) Likelihood-free inference of population structure and local adaptation in a Bayesian hierarchical model. *Genetics*, **185**, 587–602.
- Belkin M, Niyogi P (2003) Laplacian eigenmaps for dimensionality reduction and data representation. *Neural Computation*, **15**, 1373–1396.
- Benjamini Y, Hochberg Y (1995) Controlling the false discovery rate: a practical and powerful approach to multiple testing. *Journal of the Royal Statistical Society*, **57**, 289–300.

- Cai D, He X, Han J, Huang TS (2011) Graph regularized nonnegative matrix factorization for data representation. *IEEE Transactions on Pattern Analysis and Machine Intelligence*, **33**, 1548–1560.
- Cavalli-Sforza LL, Menozzi P, Piazza A (1994) *The History and Geography of Human Genes*. Princeton University Press, USA.
- Chen C, Durand E, Forbes F, François O (2007) Bayesian clustering algorithms ascertaining spatial population structure: a new computer program and a comparison study. *Molecular Ecology Notes*, **7**, 747–756.
- Chung FR (1997) *Spectral Graph Theory*, vol. 92 of *Regional Conference Series in Mathematics*. American Mathematical Society, USA.
- Devlin B, Roeder K (1999) Genomic control for association studies. *Biometrics*, **55**, 997–1004.
- Durand E, Jay F, Gaggiotti OE, François O (2009) Spatial inference of admixture proportions and secondary contact zones. *Molecular Biology and Evolution*, **26**, 1963–1973.
- Epperson BK (2003) *Geographical Genetics (MPB-38)*. Princeton University Press, USA.
- François O, Ancelet S, Guillot G (2006) Bayesian clustering using hidden Markov random fields in spatial population genetics. *Genetics*, **174**, 805–816.
- François O, Blum MG, Jakobsson M, Rosenberg NA (2008) Demographic history of European populations of *Arabidopsis thaliana*. *PLoS Genetics*, **4**, e1000075.
- François O, Durand E (2010) Spatially explicit Bayesian clustering models in population genetics. *Molecular Ecology Resources*, **10**, 773–784.
- Frichot E, François O (2015) LEA: an R package for Landscape and Ecological Association studies. *Methods in Ecology and Evolution*, **6**, 925–929.
- Frichot E, Mathieu F, Trouillon T, Bouchard G, François O (2014) Fast and efficient estimation of individual ancestry coefficients. *Genetics*, **196**, 973–983.

- Holsinger KE, Weir BS (2009) Genetics in geographically structured populations: defining, estimating and interpreting F_{st} . *Nature Reviews Genetics*, **10**, 639–650.
- Hudson RR (2002) Generating samples under a Wright–Fisher neutral model of genetic variation. *Bioinformatics*, **18**, 337–338.
- Jay F, Manel S, Alvarez N, et al (2012) Forecasting changes in population genetic structure of alpine plants in response to global warming. *Molecular Ecology*, **21**, 2354–2368.
- Kim J, Park H (2011) Fast nonnegative matrix factorization: an active-set-like method and comparisons. *SIAM Journal on Scientific Computing*, **33**, 3261–3281.
- Kimura M, Weiss GH (1964) The stepping stone model of population structure and the decrease of genetic correlation with distance. *Genetics*, **49**, 561.
- Malécot G (1948) *Les Mathématiques de l'Hérédité*. Masson, Paris.
- Manel S, Joost S, Epperson BK, et al (2010) Perspectives on the use of landscape genetics to detect genetic adaptive variation in the field. *Molecular Ecology*, **19**, 3760–3772.
- Mochizuki S, Harada A, Inada S, et al (2005) The *Arabidopsis* WAVY GROWTH 2 protein modulates root bending in response to environmental stimuli. *The Plant Cell*, **17**, 537–547.
- Pritchard JK, Stephens M, Donnelly P (2000) Inference of population structure using multilocus genotype data. *Genetics*, **155**, 945–959.
- Raj A, Stephens M, Pritchard JK (2014) fastSTRUCTURE: variational inference of population structure in large SNP data sets. *Genetics*, **197**, 573–589.
- Segelbacher G, Cushman SA, Epperson BK, et al (2010) Applications of landscape genetics in conservation biology: concepts and challenges. *Conservation Genetics*, **11**, 375–385.
- Weir (1996) *Genetic Data Analysis II*. Sinauer Associates Inc., Sunderland, MA.
- Wollstein A, Lao O (2015) Detecting individual ancestry in the human genome. *Investigative Genetics*, **6**, 1–12.
- Wright S (1943) Isolation by distance. *Genetics*, **28**, 114.

Appendix

This section provides a detailed description of the TESS3 algorithm. The first step of the algorithm builds a nearest-neighbor graph based on the geographic coordinates of the sampling sites. The number of neighbors in the graph was set to represent 5% of total connections. Then, the program runs a least-squares minimization algorithm. In this approach, the estimates of Q and G are obtained after solving the following constrained least-squares problem (Cai *et al*, 2011)

$$(\hat{Q}, \hat{G}) = \arg \min \text{LS}(Q, G),$$

where

$$\text{LS}(Q, G) = \|\tilde{X} - QG\|_{\text{F}}^2 + \alpha \sum_{s_i \sim s_j} w_{ij} \|Q_{i\cdot} - Q_{j\cdot}\|^2, \quad (1)$$

and Q and G are non-negative matrices such that, for all i and ℓ , we have

$$\sum_{k=1}^K Q_{ik} = 1 \quad \sum_{j=0}^p G_{i\ell}(j) = 1.$$

In this equation, $\|M\|_{\text{F}}$ denotes the Frobenius norm of a matrix M , $\|V\|$ is the Euclidean norm of a vector V , α is a non-negative *regularization parameter*. The summation on the right-hand side of the second term runs over all pairs of sites, $s_i \sim s_j$, sharing an edge in the nearest-neighbor graph. The quantity w_{ij} is a weight that decreases with geographic distance between sampling sites as follows

$$w_{ij} = \exp(-d(s_i, s_j)^2/\bar{d}^2), \quad (2)$$

where d is the Euclidean distance, and \bar{d} is the average distance computed over the neighboring sites in the sample. More specifically, the weight of an edge in the nearest-neighbor graph is related to the Laplace-Beltrami operator on a manifold (Belkin & Niyogi, 2003). In the algorithm, the regularization parameter α is equal to $c \times nL(p+1)/\sum w_{ij}$. The default value of c is 0.1%.

Least squares minimization is performed using the Alternating Non-negativity-constrained Least Squares (ANLS) algorithm with the active set (AS) method following the approach used in

the computer program **sNMF** (Frichot *et al.*, 2014; Kim & Park, 2011). The ANLS-AS algorithm starts with the initialization of the Q matrix, and then computes a non-negative matrix G that minimizes the quantity

$$\text{LS}_1(G) = \|X - QG\|_F^2.$$

The obtained solution is normalized so that its entries satisfy the probabilistic constraints for genotypic frequencies. Given G , the Q -matrix is computed after minimizing the following quantity

$$\text{LS}_2(Q) = \left\| \begin{pmatrix} \text{Vec}(\tilde{X}^T) \\ 0 \end{pmatrix} - \begin{pmatrix} \text{Id} \otimes G^T \\ \sqrt{\alpha} \Gamma \otimes \text{Id} \end{pmatrix} \text{Vec}(Q^T) \right\|_F^2,$$

where $\text{Vec}(\tilde{X})$ denotes the vectorization of the matrix \tilde{X} formed by stacking the columns of \tilde{X} into a single column vector, Γ is the Cholesky decomposition of the graph Laplacian associated with the weights of the graph (Chung, 1997), Id is the identity matrix, and \otimes is a symbol for the Kronecker product. Iterations are stopped when the relative difference between two successive values of $\text{LS}(Q, G)$ is lower than a tolerance threshold of ϵ . The default value for ϵ equals 10^{-7} .

5 Figures and Tables

Figure 1. Statistical errors of TESS3 and TESS 2.3 estimates. Computer simulations of admixed populations using known individual ancestry proportions from two ancestral gene pools. A) RMSEs of G estimates as a function of the level of ancestral population differentiation (F_{ST}). B) RMSEs of Q estimates as a function of the level of ancestral population differentiation (F_{ST}).

Figure 2. Run-times for TESS3 and TESS 2.3. The number of ancestral population ranged between $K = 1$ and 6. Run-times were expressed in unit of minutes.

Figure 3. Results of the *Arabidopsis thaliana* data analysis with TESS3. A) Geographic maps of ancestry coefficients using $K = 3$ ancestral populations. B) Manhattan plot of $\log_{10}(p\text{-values})$ for the plant chromosome 5. The horizontal line corresponds to an expected FDR value of $q = 10^{-30}$.

Figure 4. Candidate SNPs from a genome scan of *A. thaliana* chromosome 5. A) Histogram of adjusted p -values. B) Spatial distribution of allele frequency for two top-hit SNPs located in the *VSP1* and *WAV2* genes.

Table1. Power to reject neutrality of TESS3 outlier tests for two simulated data sets.

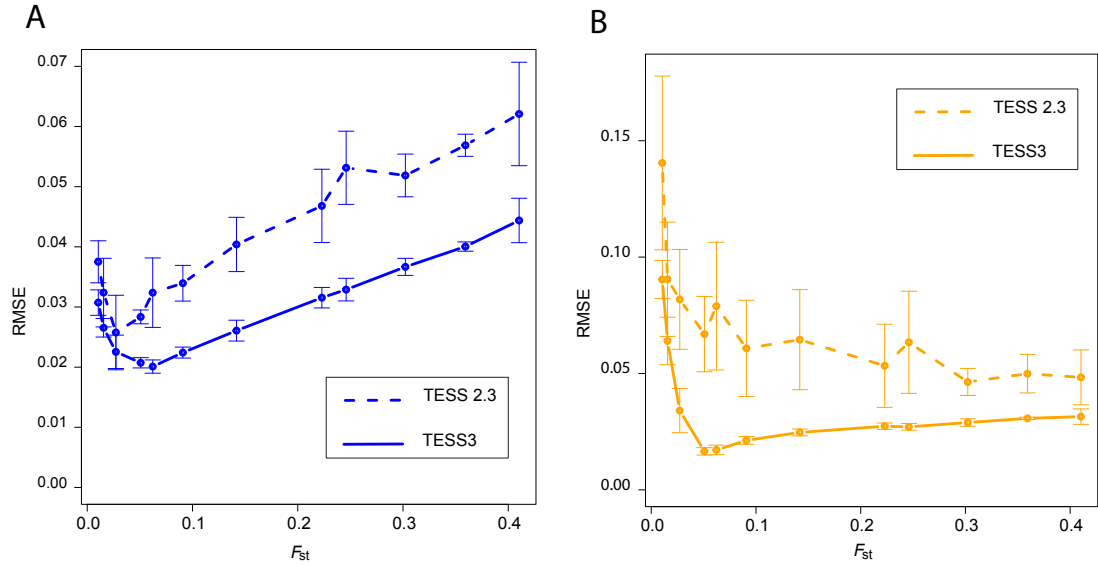


Figure 1: Statistical errors of TESS3 and TESS 2.3 estimates. Computer simulations of admixed populations using known individual ancestry proportions from two ancestral gene pools. A) RMSEs of G estimates as a function of the level of ancestral population differentiation (F_{ST}). B) RMSEs of Q estimates as a function of the level of ancestral population differentiation (F_{ST}).

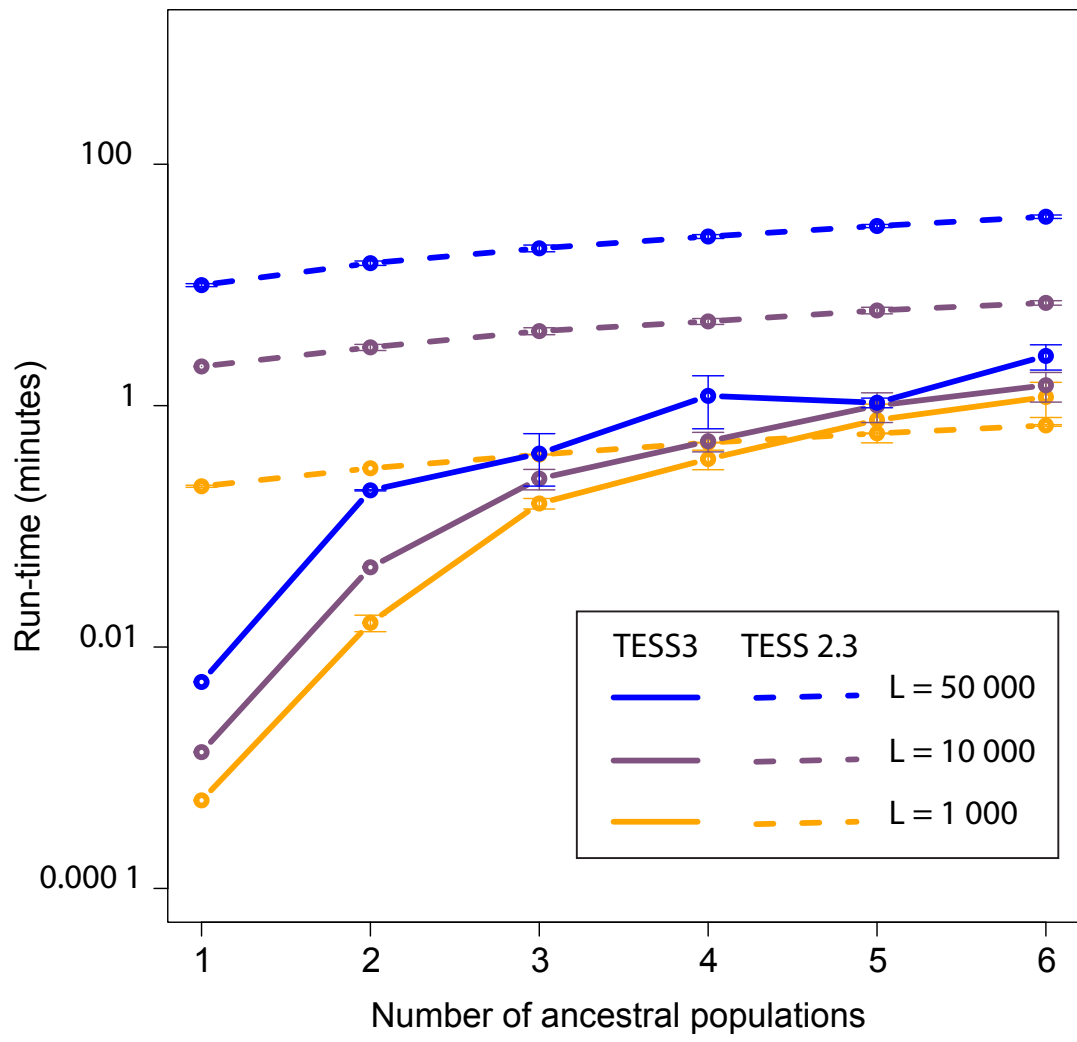


Figure 2: Run-times for TESS3 and TESS 2.3. The number of ancestral population ranged between $K = 1$ and 6. Run-times were expressed in unit of minutes.

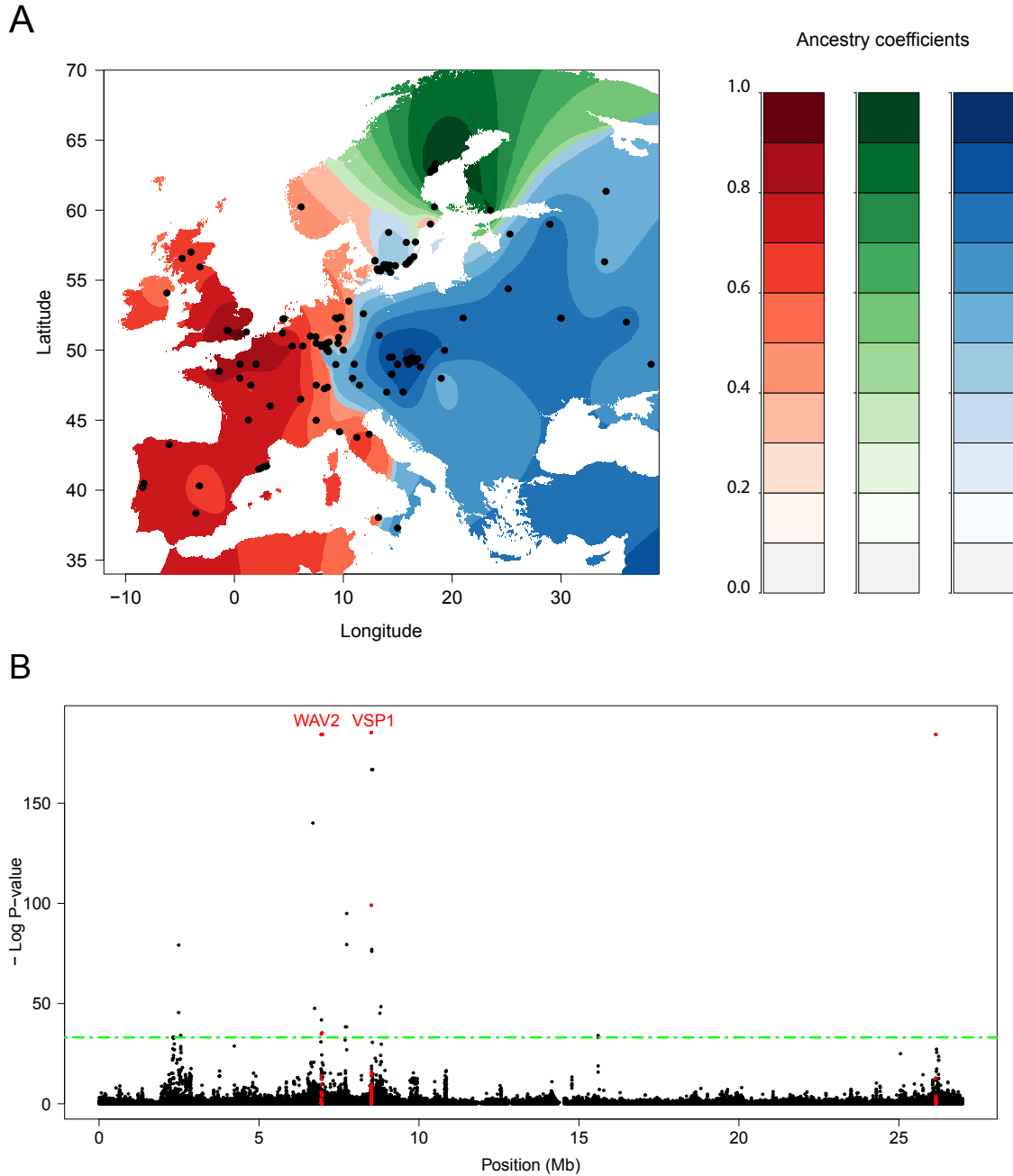
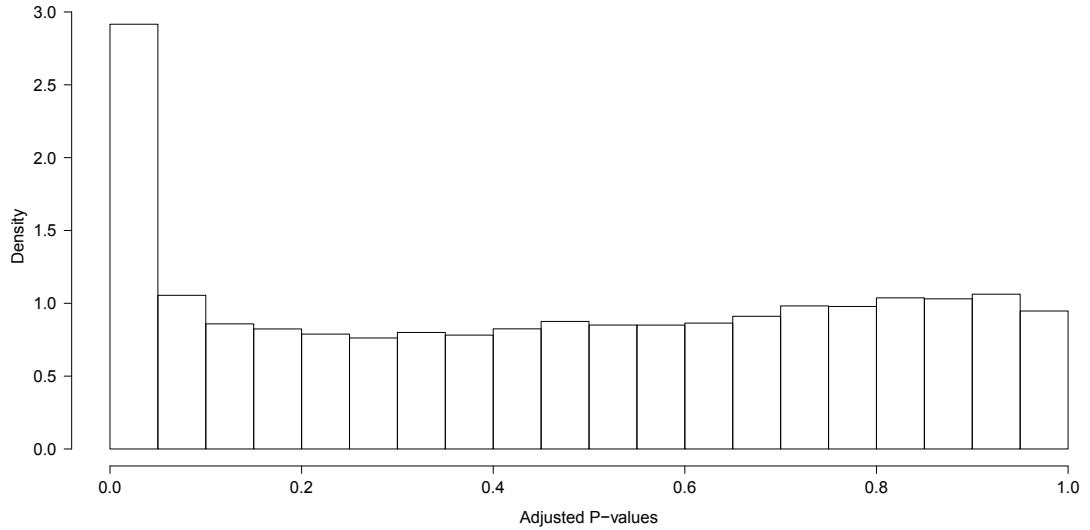


Figure 3: Results of the *Arabidopsis thaliana* data analysis with TESS3. A) Geographic maps of ancestry coefficients using $K = 3$ ancestral populations. B) Manhattan plot of $\log_{10}(p\text{-values})$ for the plant chromosome 5. The horizontal line corresponds to an expected FDR value of $q = 10^{-30}$.

A



B

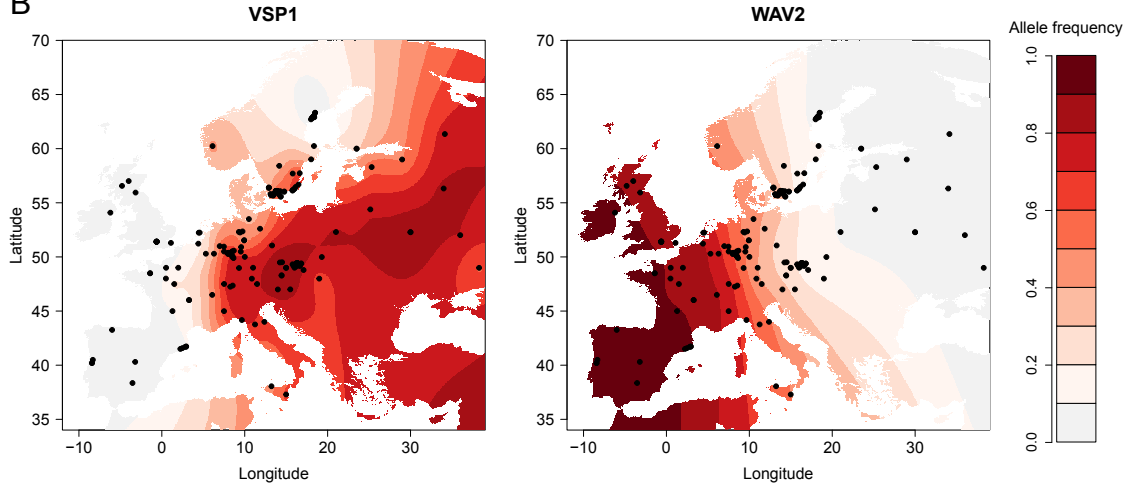


Figure 4: Candidate SNPs from a genome scan of the *A. thaliana* 5th chromosome. A) Histogram of adjusted p -values. B) Spatial distribution of allele frequency for two top-hit SNPs located in the *VSP1* and *WAV2* genes.

Table1. Power to reject neutrality of TESS3 outlier tests for two simulated data sets.

| FDR | Power | | | |
|------|-----------------|------------------|-----------------|------------------|
| | After admixture | Before admixture | After admixture | Before admixture |
| 0.05 | 0.61 | 0.63 | 0.20 | 0.26 |
| 0.10 | 0.63 | 0.66 | 0.23 | 0.29 |
| 0.15 | 0.64 | 0.67 | 0.25 | 0.32 |
| 0.20 | 0.65 | 0.69 | 0.26 | 0.33 |

Data set 1: $m_s/m = 0.005$. Data set 2: $m_s/m = 0.05$.